Supporting Information

for

Long Aliphatic Chain Derivatives of Trigonal Lanthanide Complexes

*Yiwei Zhou, Christian D. Buch, Steen H. Hansen and Stergios Piligkos**

Department of Chemistry, University of Copenhagen, Universitetsparken 5, DK-2100 Copenhagen (Denmark)

E-mail:piligkos@chem.ku.dk

Contents

Mass spectra....2
Infrared spectroscopy....4
NMR spectrum....9
Powder X-ray diffraction....10
Crystallographic Table....12
Crystal structures....13
Magnetic susceptibility....20
Variable-temperature-variable-field measurements....21
Ac susceptibility....22

Mass spectra

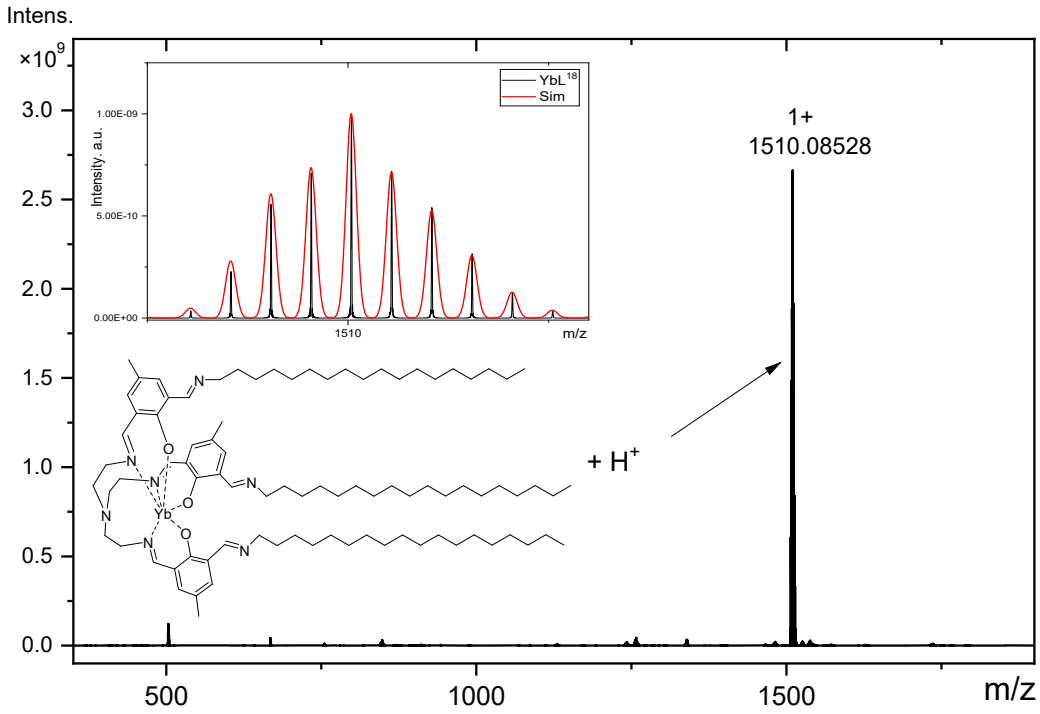

Figure S1. Positive ion mode MALDI mass spectrum of **1**.

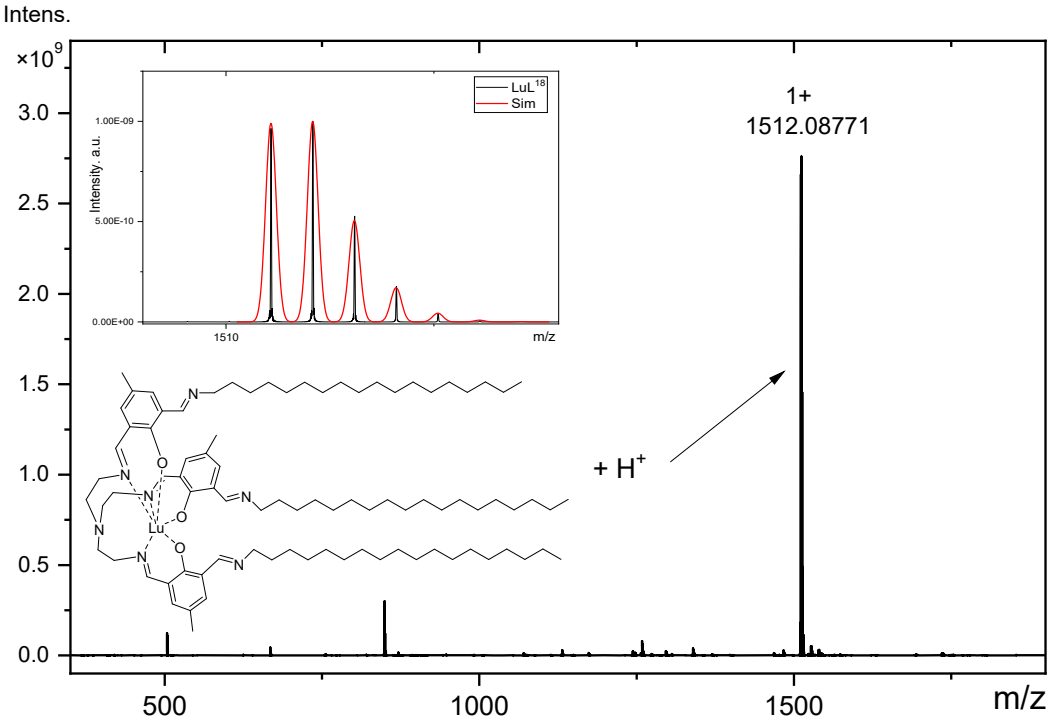

Figure S2. Positive ion mode MALDI mass spectrum of **2**.

Infrared spectroscopy

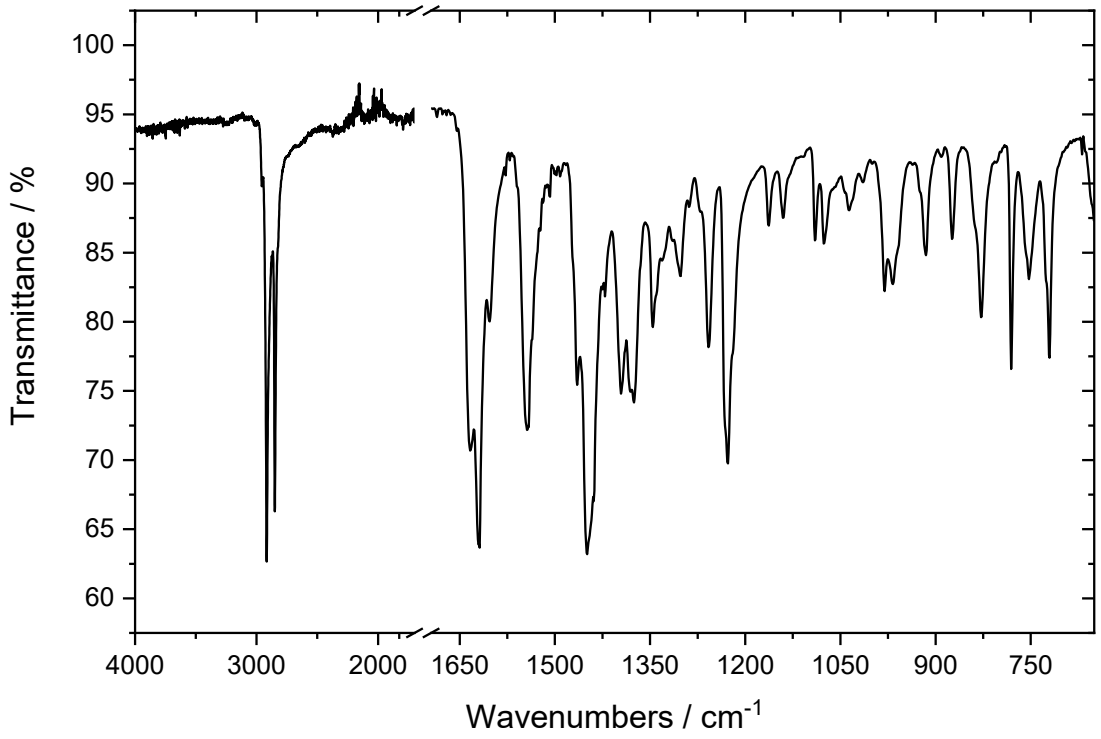

Figure S3. FTIR spectrum of **1**.

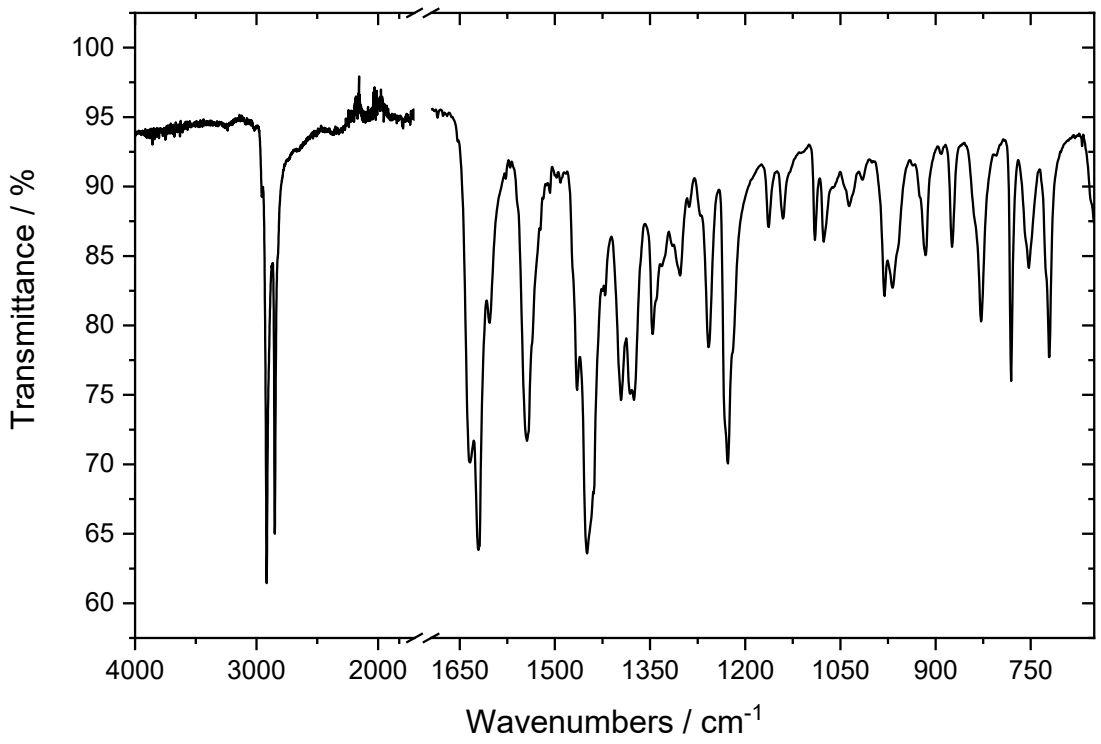

Figure S4. FTIR spectrum of **2**.

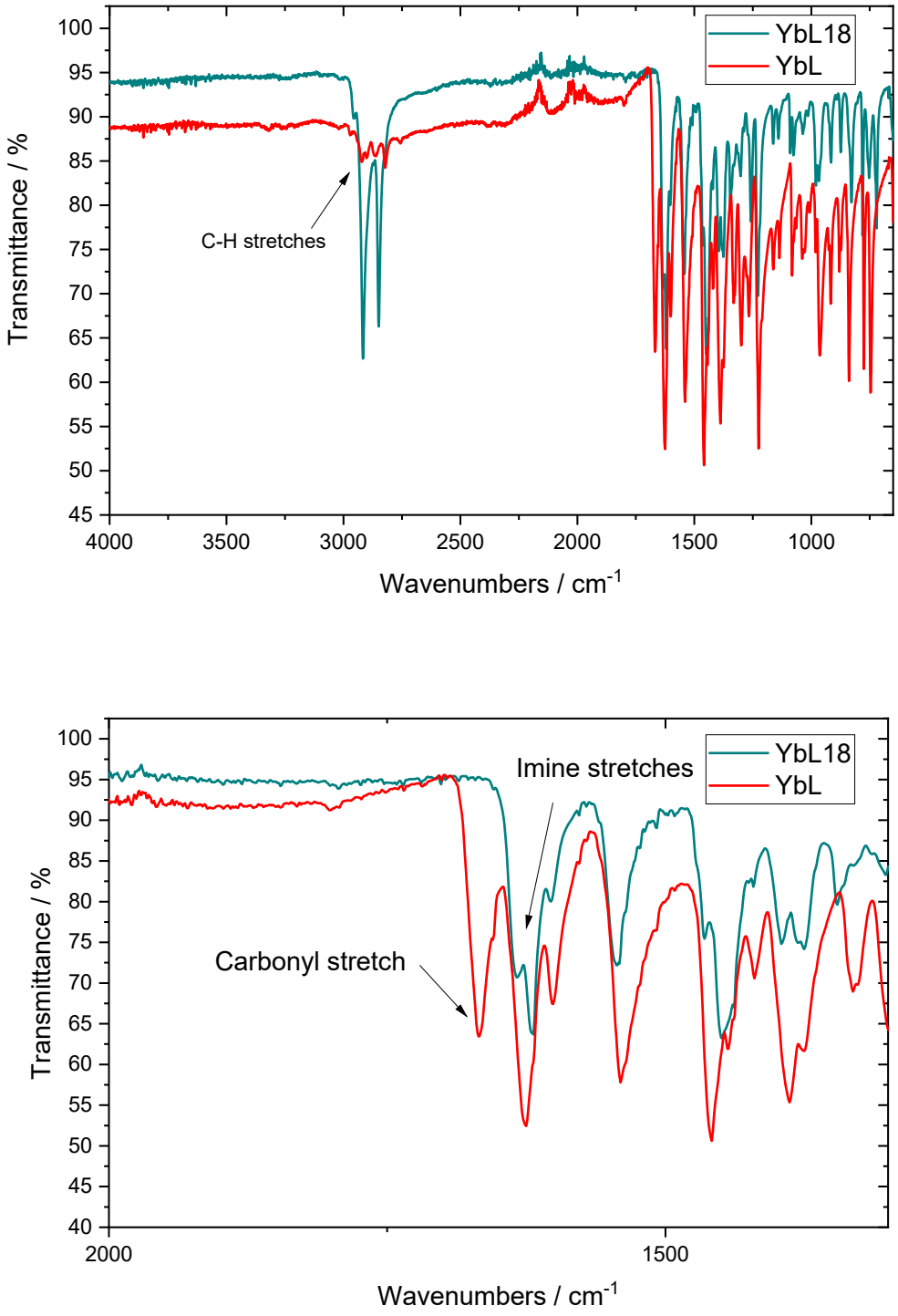

Figure S5. Top: FTIR spectra of a polycrystalline powder of **1** (cyan) and of a polycrystalline powder of **YbL** (red). Bottom: Enlargement of the range 2000-1300 cm^{-1} of the FTIR spectra of a polycrystalline powder of **1** (cyan) and of a polycrystalline powder of **YbL** (red).

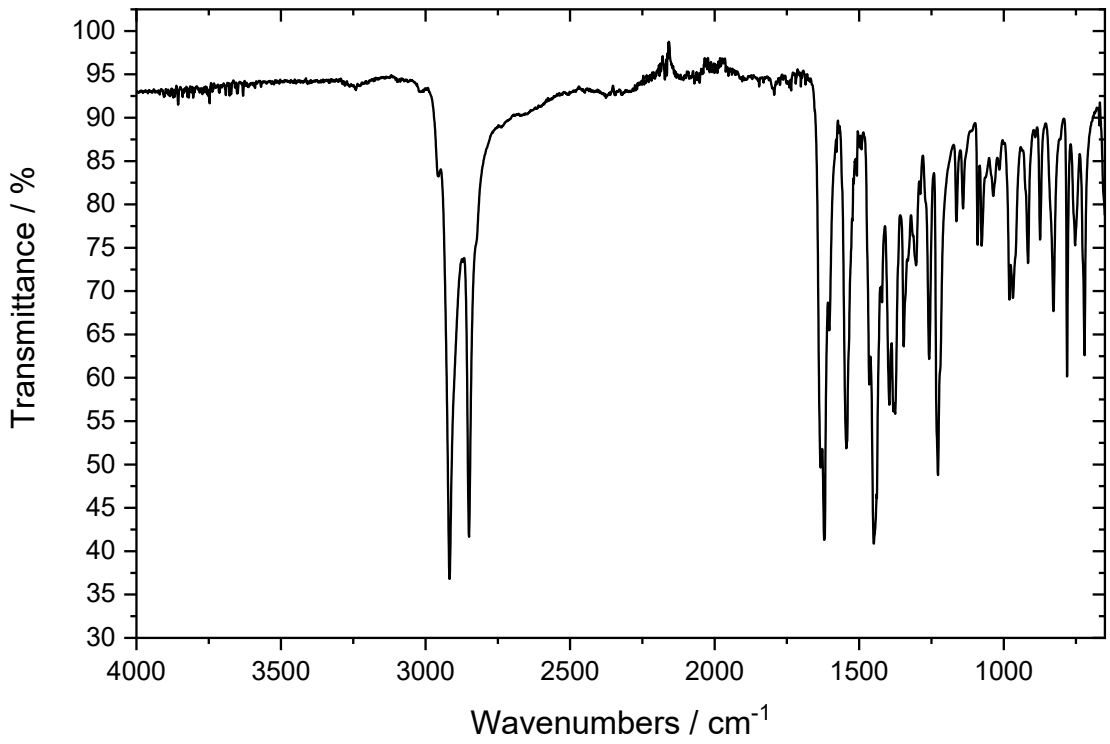

Figure S6. FTIR spectrum of **1'**.

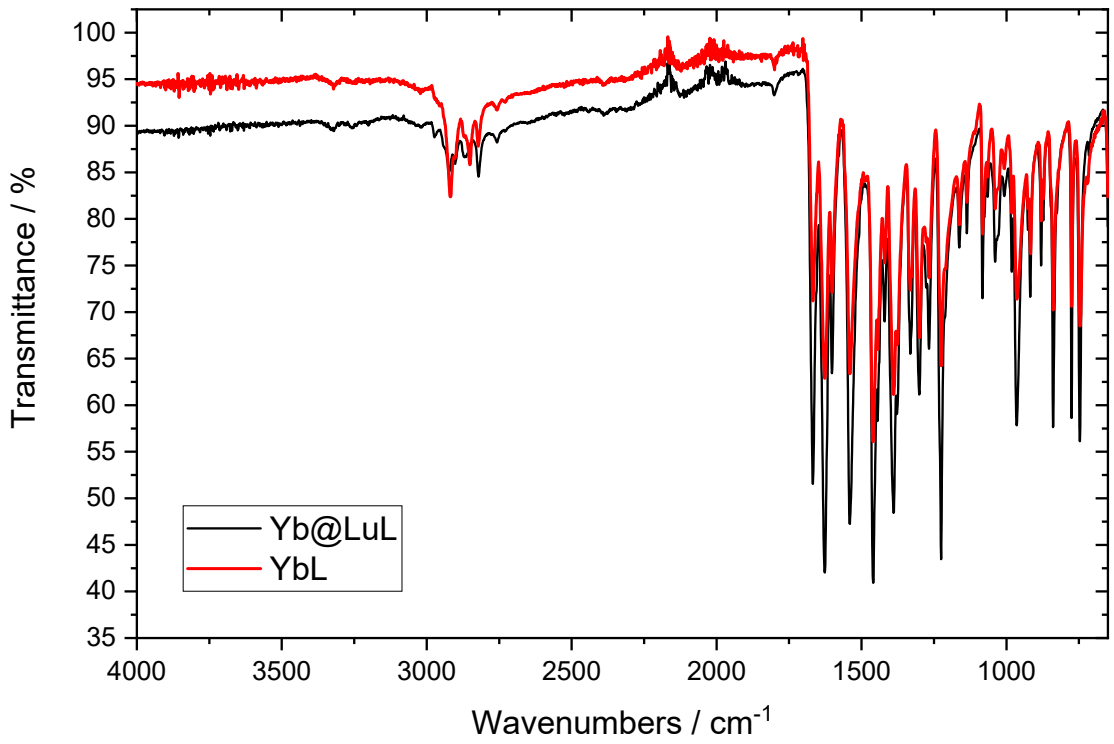

Figure S7. FTIR spectra of **Yb@LuL** at 4.2% dilution and **YbL**.

NMR spectrum

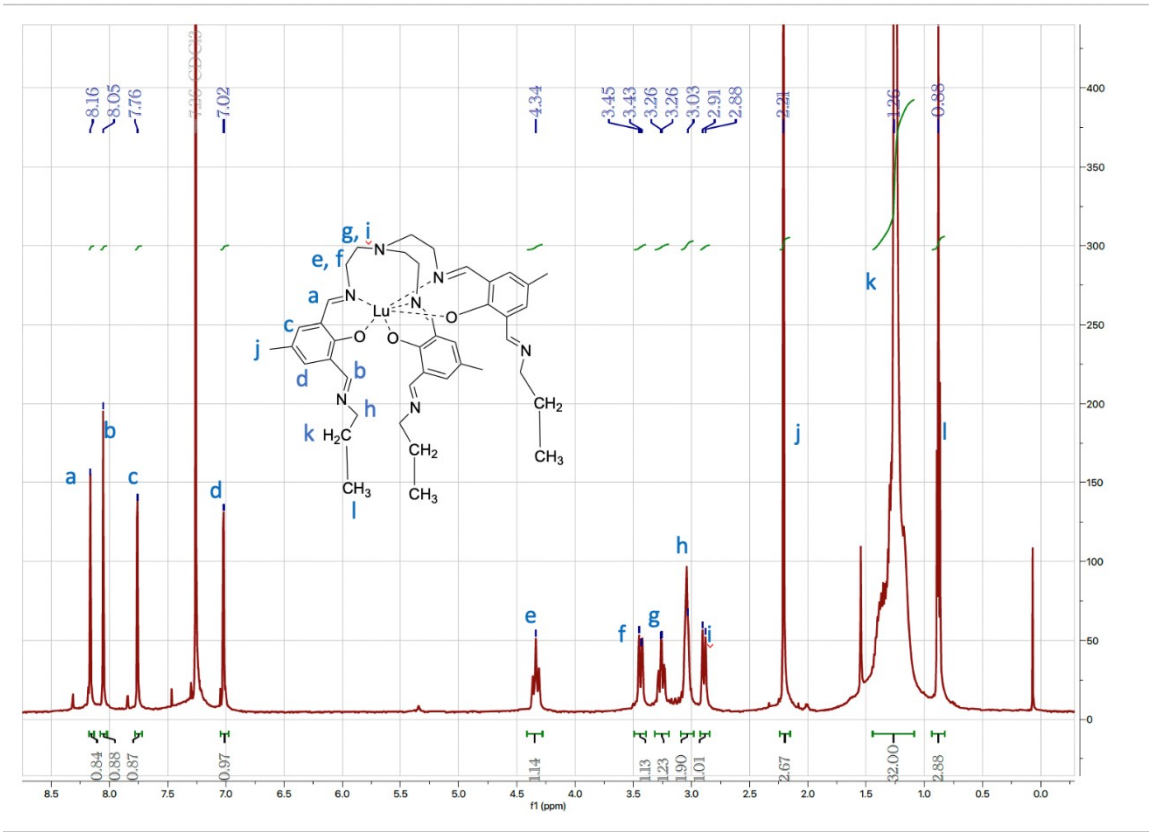

Figure S8. ^{1}H NMR of **2** in deuterated $CDCl_3$, the peak at 1.55 ppm is from water in the $CDCl_3$ and the signal at 7.26 is from the deuterated solvent.

Powder X-ray diffraction

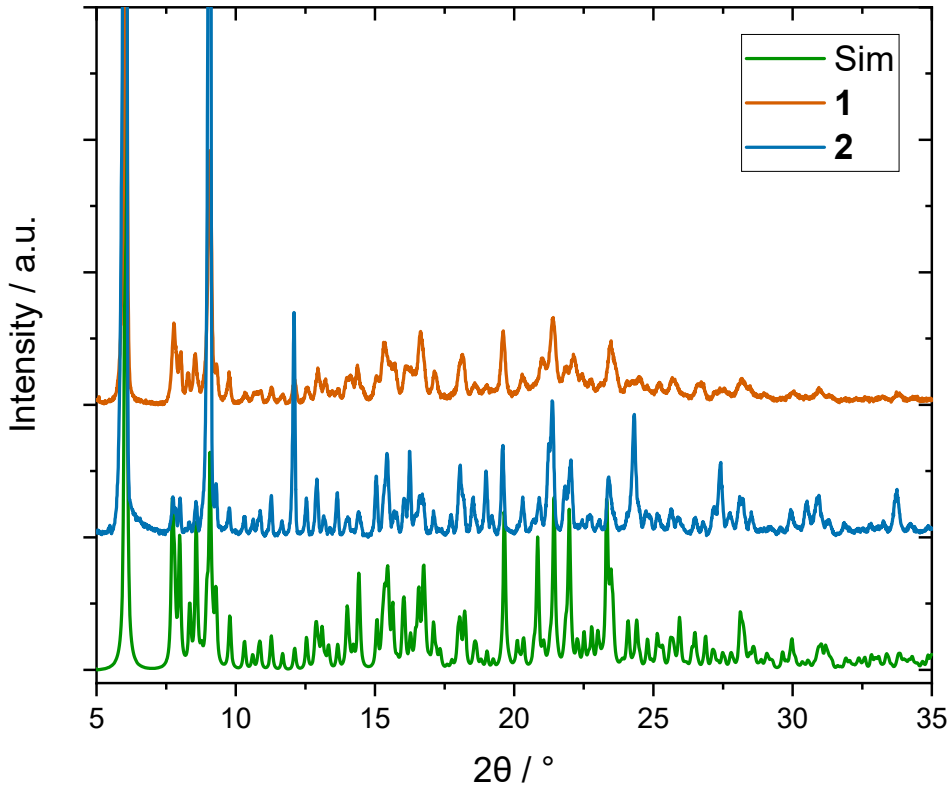

Figure S9. PXRD data for **1** and **2**. The simulated PXRD pattern was calculated from a crystal structure measured at room temperature.

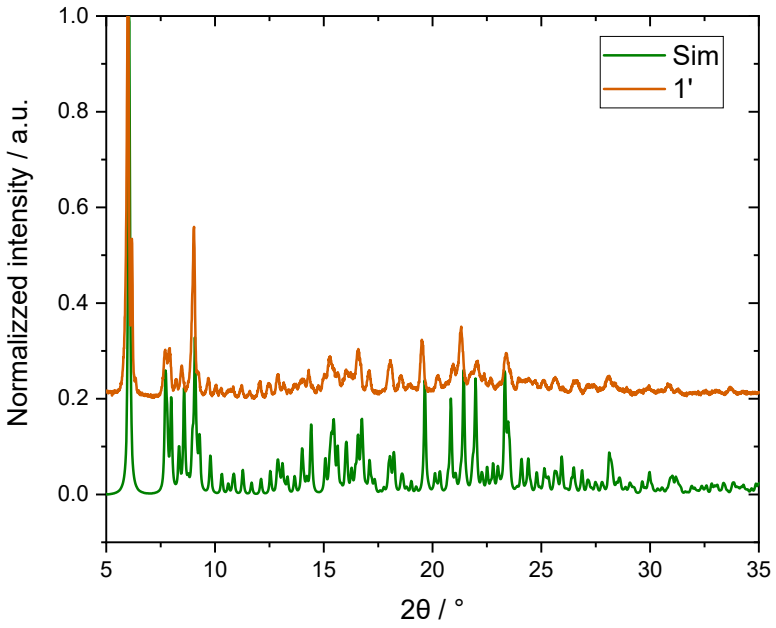

Figure S10. PXRD of **1'** complex. The simulated PXRD pattern was calculated from a crystal structure measured at room temperature.

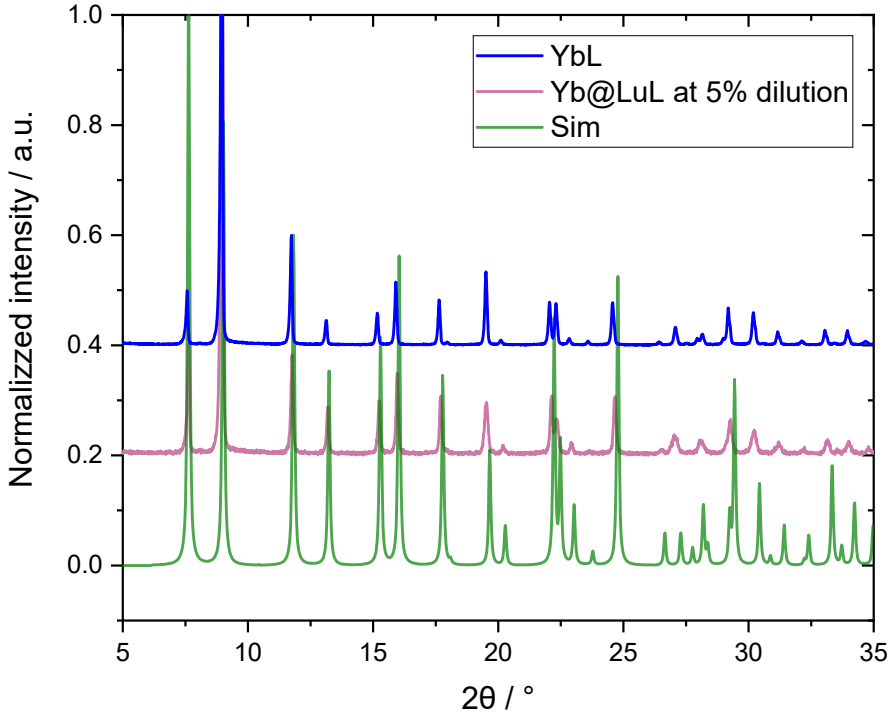

Figure S11. PXRD of **YbL** and **Yb@LuL** at 4.2% dilution. The simulated PXRD pattern was calculated from a crystal structure measured at room temperature.

Crystallographic Table

Table S1: Crystallographic data of **1**.

Complex	**1**
Empirical formula	$C_{87}H_{144}N_7O_3Yb$
Formula weight	1509.12
Temperature/K	100
Crystal system	Triclinic
Space group	$P\bar{1}$
***a*/Å**	12.4294(8)
***b*/Å**	12.4635(8)
***c*/Å**	30.023(2)
***α*/°**	91.216(2)
***β*/°**	98.672(2)
***γ*/°**	115.930(2)
Volume/Å^3	4115.0(5)
Z	2
ρ_{calc} g/cm^3	1.218
μ/mm^{-1}	1.187
F (000)	1618.0
Crystal size/mm^3	0.43 × 0.183 × 0.05
λ (MoKα)	0.71073
2Θ range for data collection/°	4.028 to 51.364
Index ranges	$-15 \le h \le 15$, $-15 \le k \le 15$, $-36 \le l \le 36$
Reflections collected	118800
Independent reflections	15615 [R_{int} = 0.0400, R_{sigma} = 0.0221]
Data/restraints/ parameters	15615/0/889
Goodness-of-fit on F^2	1.071
Final *R* indexes [$I>=2\sigma(I)$]	R_1 = 0.0219, wR_2 = 0.0521
Final *R* indexes [all data]	R_1 = 0.0259, wR_2 = 0.0539
Largest diff. peak/hole / e Å^{-3}	1.25/-0.74

Crystal structures

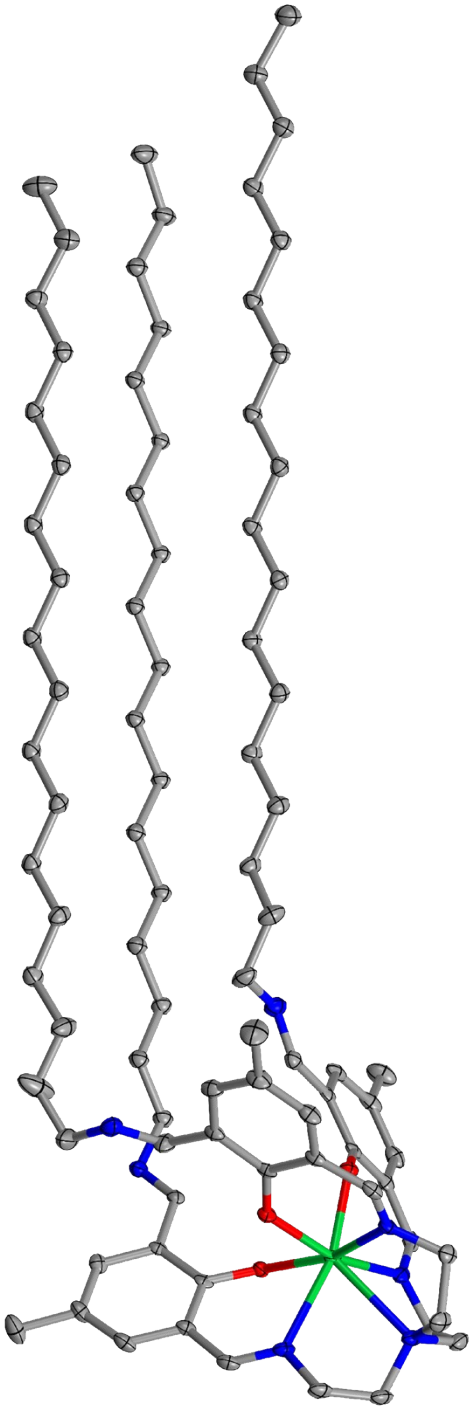

Figure S12. Solid state structure of **1** seen from the side. Colour code: Yb, green; N, blue; O, red; C, grey; H, white. All hydrogen atoms have been omitted for clarity. Thermal ellipsoids are set to 50% probability.

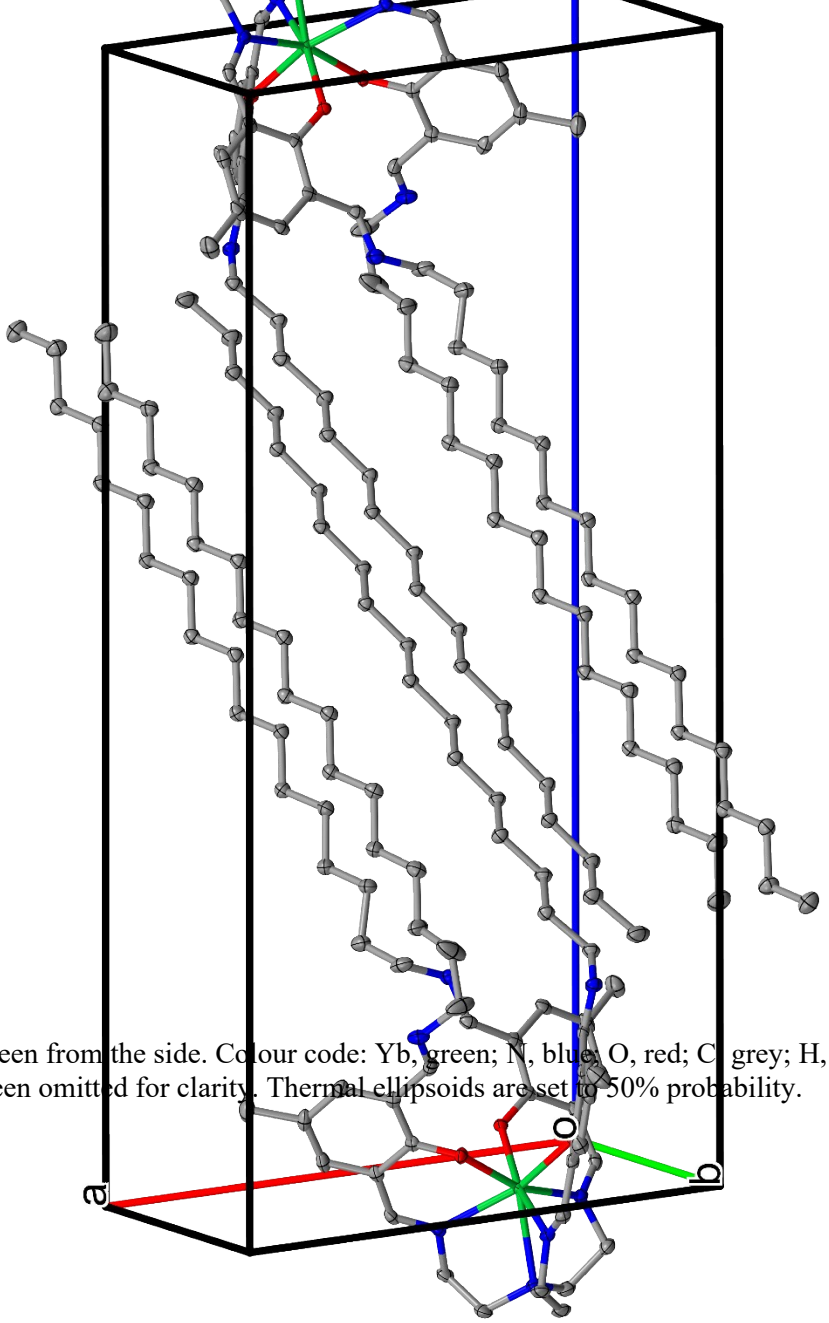

Figure S13. Unit cell of **1** seen from the side. Colour code: Yb, green; N, blue; O, red; C, grey; H, white. All hydrogen atoms have been omitted for clarity. Thermal ellipsoids are set to 50% probability.

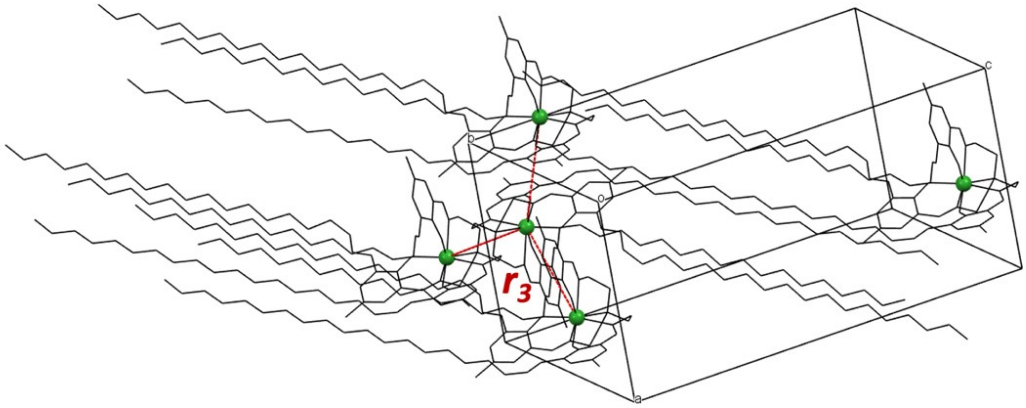

Figure S14. Illustration of the three closest neighbouring complexes in **1**.

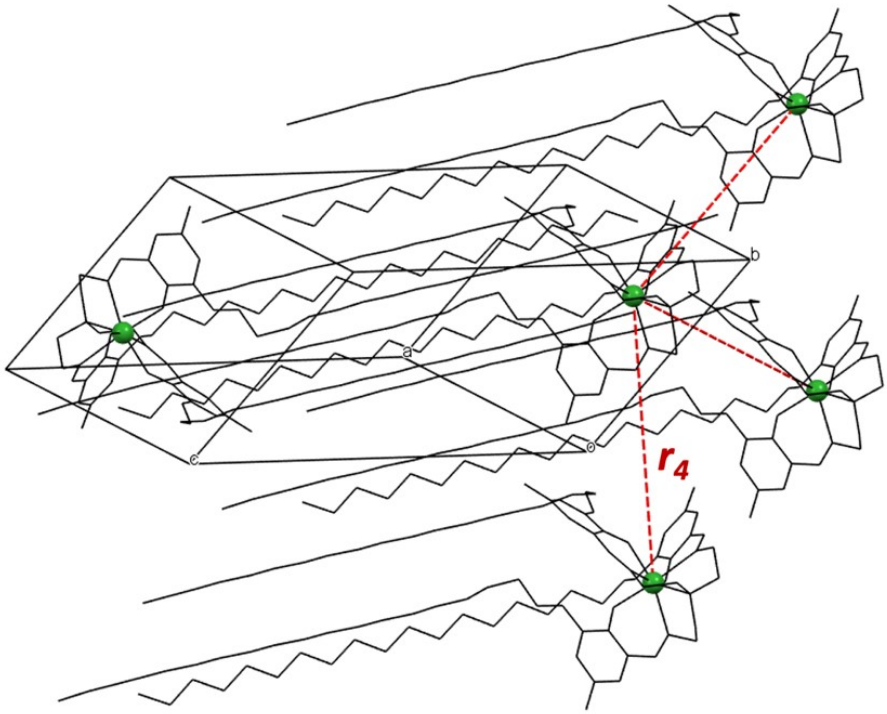

Figure S15. The distance of the closest neighbours with the chains pointing in the same direction in **1**.

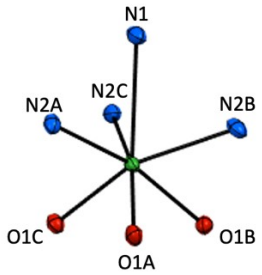

Figure S16: The distorted monocapped octahedral coordination environment around Yb(III) in **1**. Colour code: Yb, green; N, blue; O, red. Thermal ellipsoids are set to 50% probability.

Table S2. Comparison of selected bond lengths in **1**, YbL[1] and YbL derivatised with three benzylamine groups (Yb^BL)[1]. The three phenoxide and imine groups are labelled according to Figure S16.

Bond length / Å	Ln-O1A	Ln-O1B	Ln-O1C	Ln-N2A	Ln-N2B	Ln-N2C	Ln-N1
1	2.1511(14)	2.1552(13)	2.1629(13)	2.4173(16)	2.4179 (16)	2.4194(17)	2.6124(16)
YbL	2.1600(15)	2.1600(15)	2.1600(15)	2.421(1)	2.421(1)	2.421(1)	2.610(3)
Yb^BL	2.1428(12)	2.1590(16)	2.1663(16)	2.422(2)	2.423(2)	2.4259(16)	2.616(2)

Table S3. Comparison of selected bond angles of **1**, YbL[1] and YbL derivatised with three benzylamine groups (Yb^BL)[1]. The three phenoxide and imine groups are labelled according to Figure S16.

Bond angle / °	∠N2A-N2B-N2C	∠N2B-N2A-N2C	∠N2A-N2C-N2B	∠N1-Ln-N2A	∠N1-Ln-N2B	∠N1-Ln-N2C	∠N1-Ln-O1A	∠N1-Ln-O1B	∠N1-Ln-O1C	∠O1A-O1B-O1C	∠O1B-O1A-O1C	∠O1A-O1C-O1B
1	61.34(5)	61.03(5)	57.62(5)	69.17(5)	69.19(5)	69.18(5)	127.97(6)	125.20(5)	127.42(5)	59.74(3)	61.11(3)	59.15(5)
YbL	60.00	60.00	60.00	69.27(4)	69.27(4)	69.27(4)	127.02(4)	127.02(4)	127.02(4)	60.00	60.00	60.00
Yb^BL	57.11(5)	61.26(5)	61.63(5)	68.96(7)	68.53(7)	69.37(7)	130.21(6)	125.20(7)	126.18(7)	59.09(5)	62.96(5)	57.95(5)

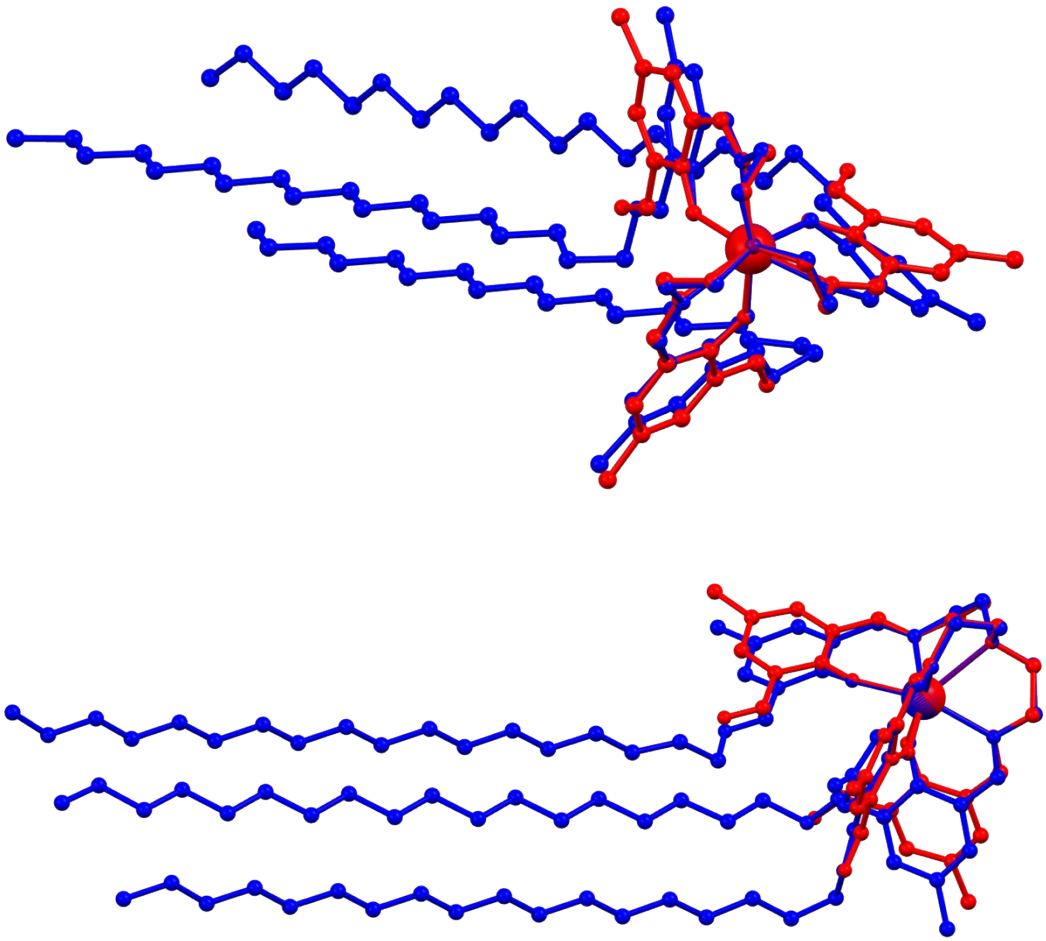

Figure S17. Structural overlay of **1** (blue) and YbL (red) seen from the top (top) and from the side (bottom). The crystal structure of YbL was obtained from literature.[1]

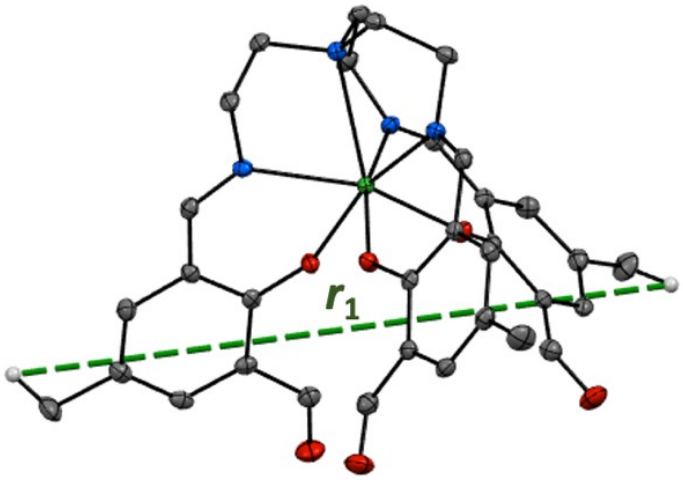

Figure S18. Solid state structure of **YbL** showing the longest intra molecular distance, r_1. Hydrogen atoms have been omitted for clarity except for the hydrogens which are part of r_1. Colour code: Yb, green; N, blue; O, red; C, grey; H, white. Thermal ellipsoids are set to 50% probability.

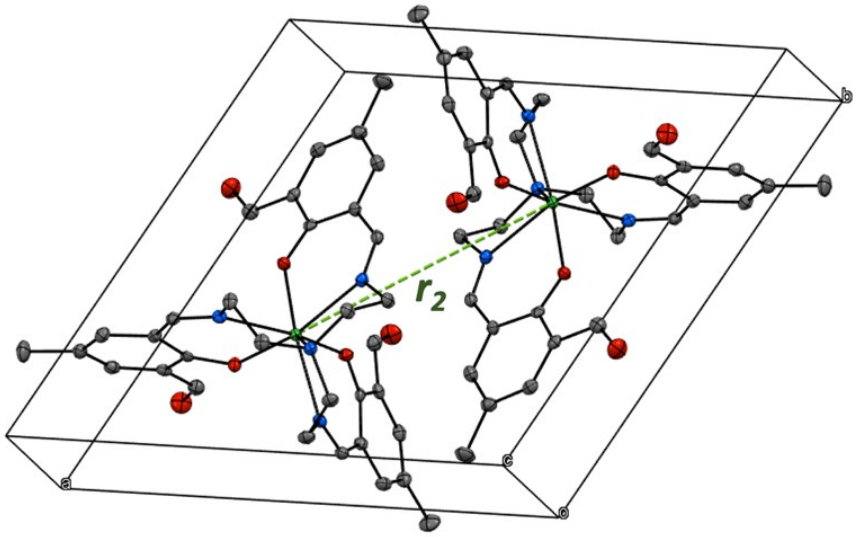

Figure S19. Unit cell of **YbL** with the distance between the two Yb(III) centres (r_2). Hydrogen atoms have been omitted for clarity. Colour code: Yb, green; N, blue; O, red; C, grey. Thermal ellipsoids are set to 50% probability.

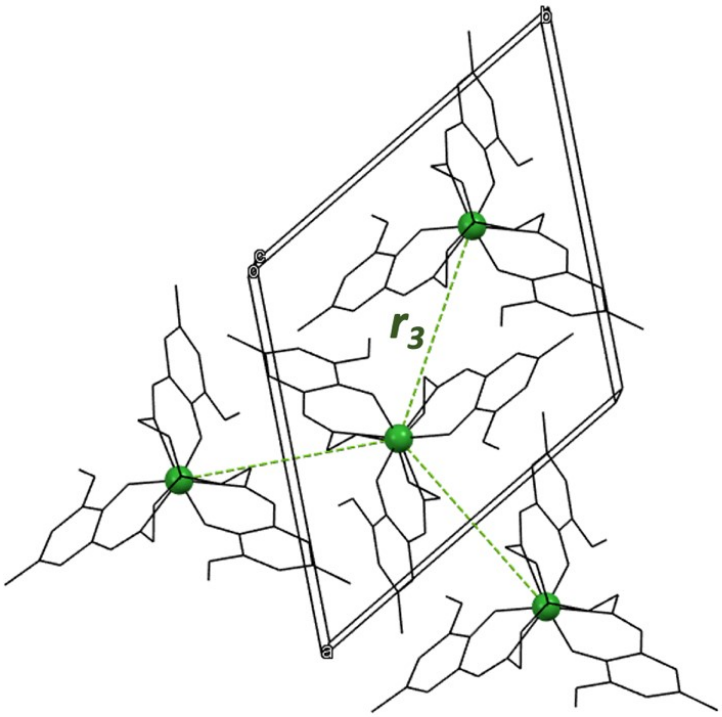

Figure S20. Illustration of the three closest neighbouring complexes in **YbL**.

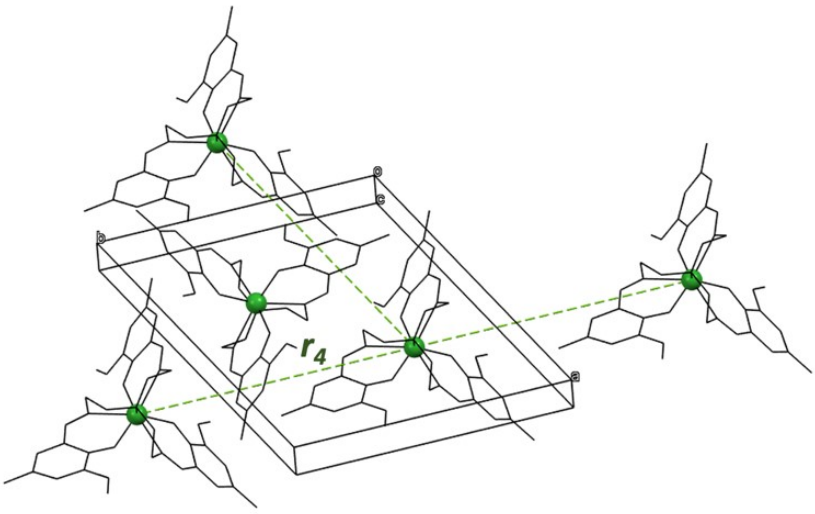

Figure S21. The distance to the closest neighbours with the chains pointing in the same direction in **YbL**.

Magnetic susceptibility

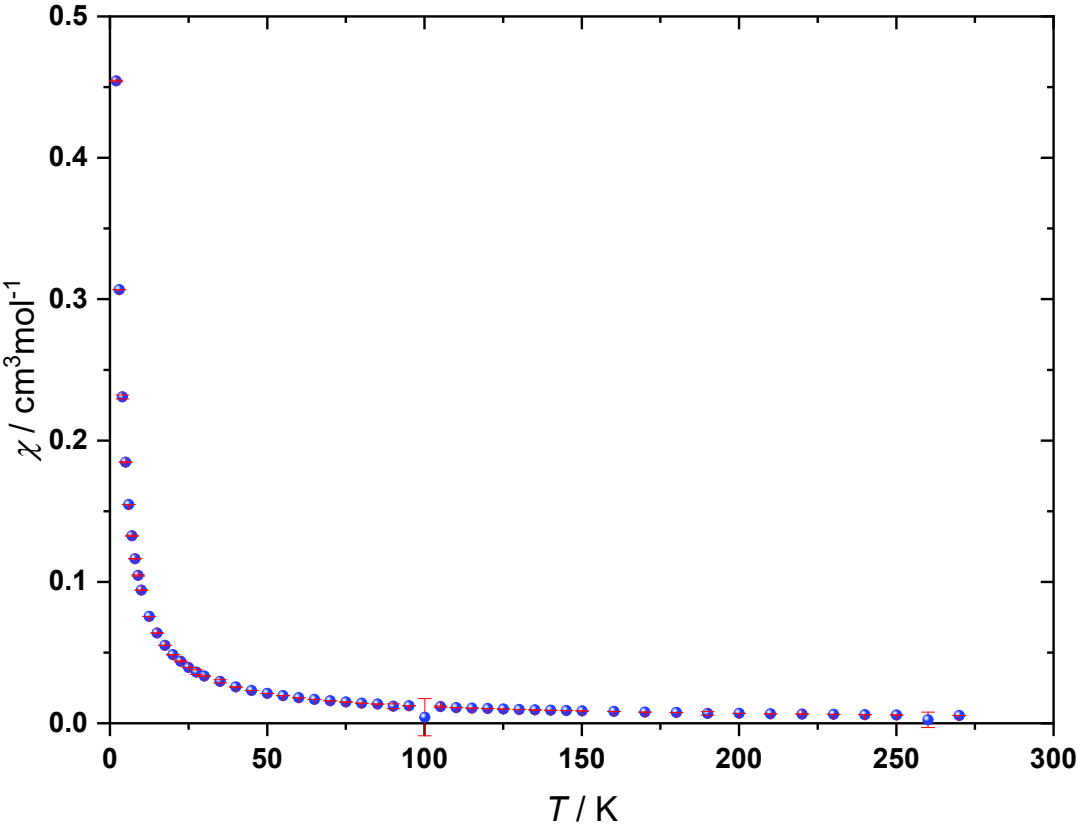

Figure S22. Temperature dependence of χ (points) including errors (red bars) for **1**.

Variable-temperature-variable-field measurements

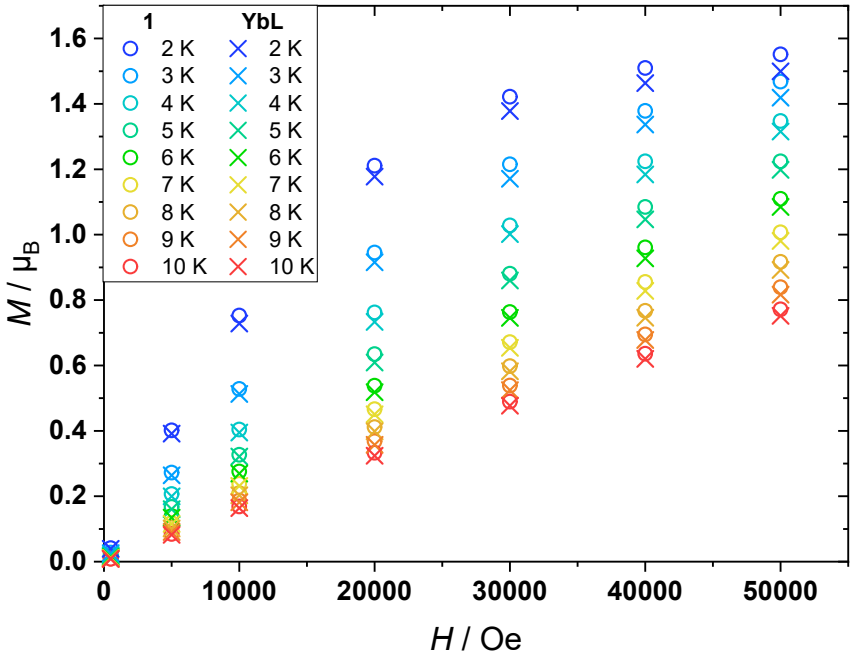

Figure S23. Comparison of VTVB measurements of **1** (circles) and YbL (crosses). The YbL values are obtained from literature.[1]

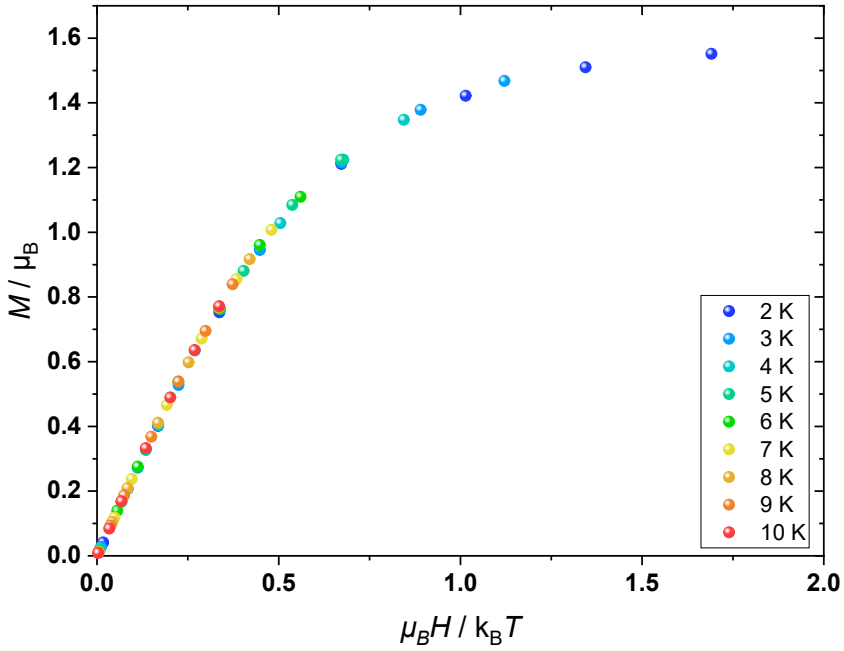

Figure S24. Reduced magnetization of **1**.

Ac susceptibility

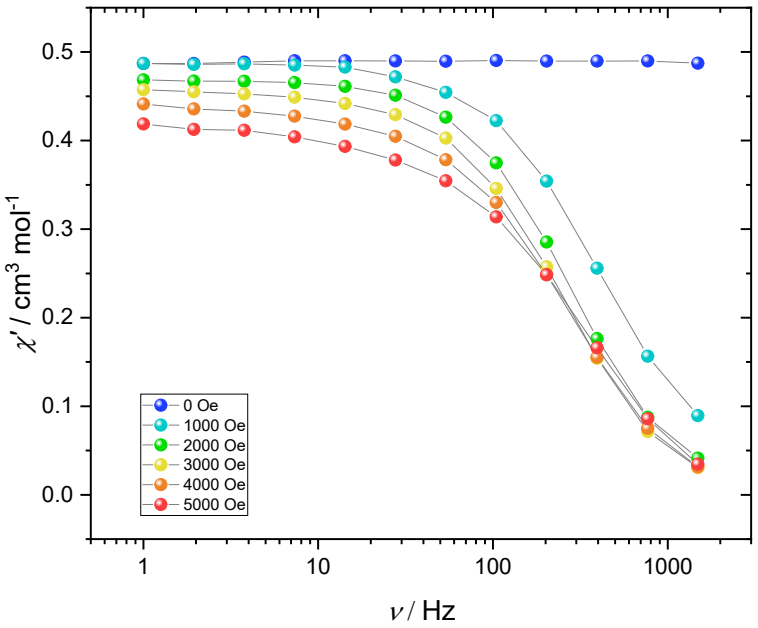

Figure S25. Field dependence of the in-phase signal of the ac magnetic susceptibility of **1**. Solid lines are guidelines for the eye.

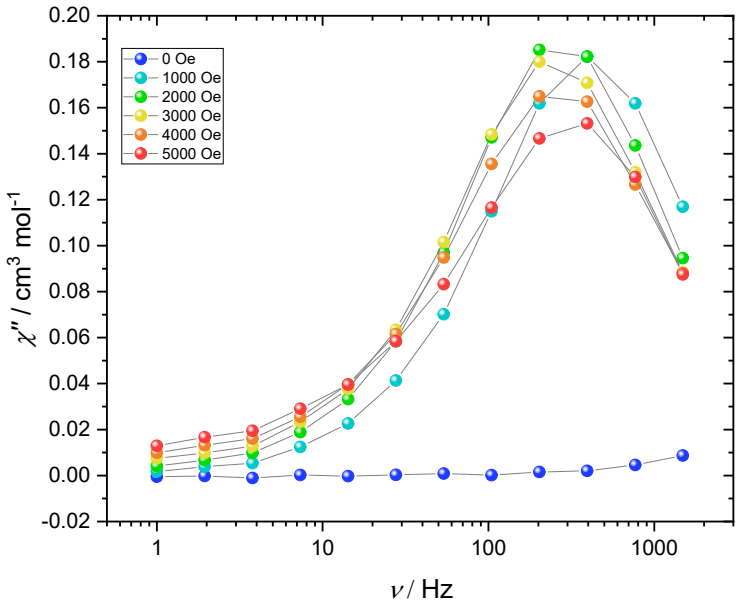

Figure S26. Field dependence of the out-of-phase signal of the ac magnetic susceptibility of **1**. Solid lines are guidelines for the eye.

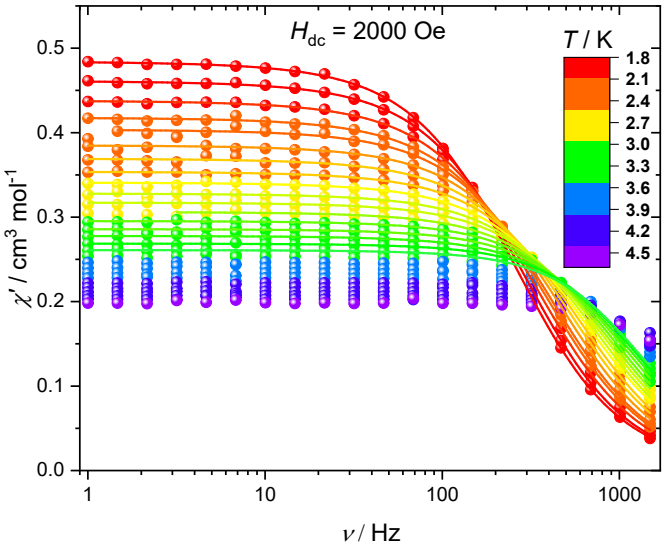

Figure S27. Temperature dependence of the in-phase signal of the ac susceptibility of **1**. Solid lines are best fits to the generalised Debye model as described in the main text. Parameters can be found in Table S4.

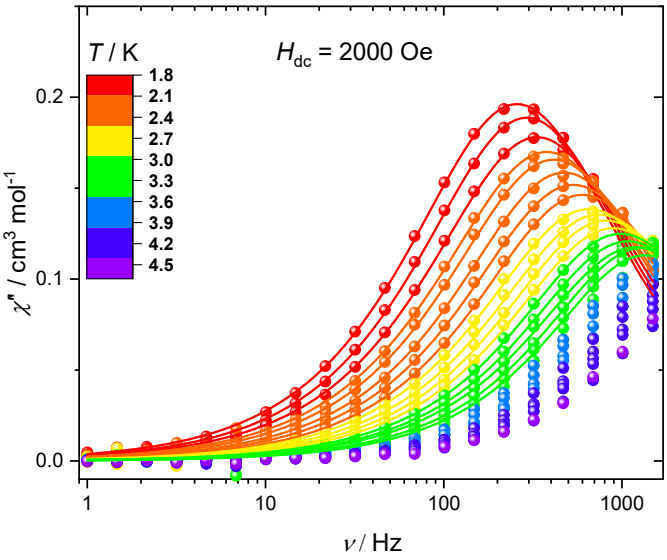

Figure S28. Temperature dependence of the out-of-phase signal of the ac susceptibility of **1**. Solid lines are best fits to the generalised Debye model as described in the main text. Parameters can be found in Table S4.

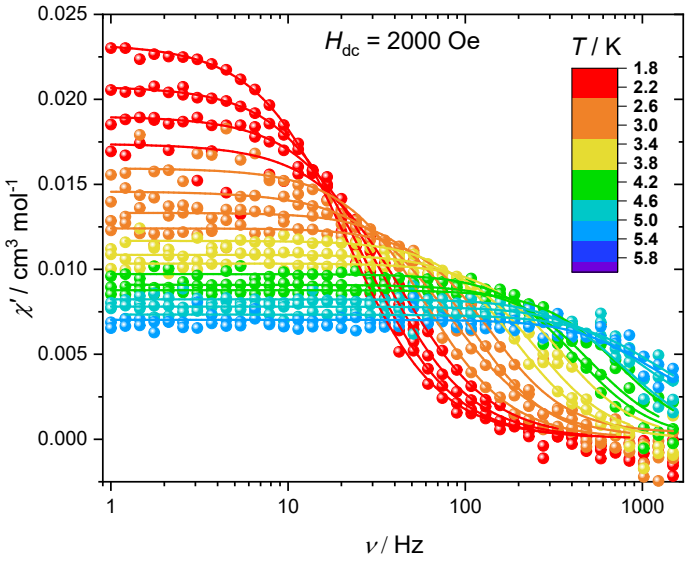

Figure S29. Temperature dependence of the in-phase signal of the ac susceptibility of **1'** at 4.8 % dilution. Solid lines are best fits to the generalised Debye model as described in the main text. Parameters can be found in Table S5.

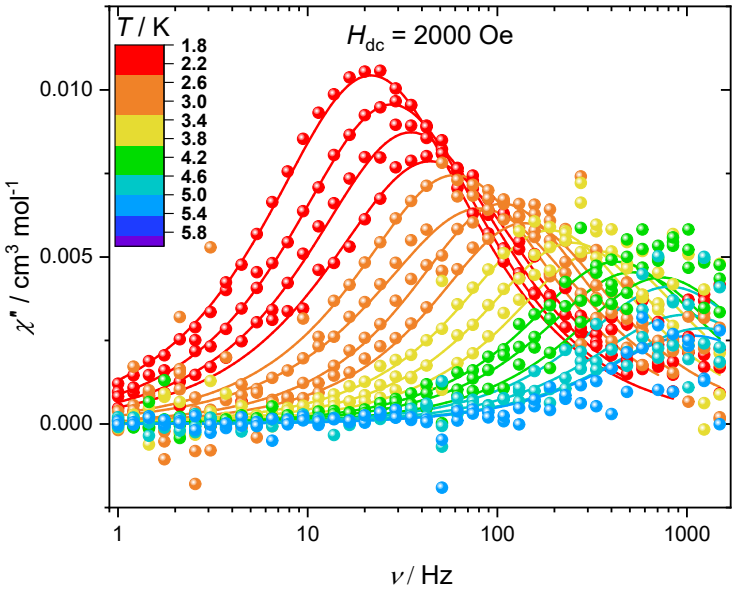

Figure S30. Temperature dependence of the out-of-phase signal of the ac susceptibility of **1'** at 4.8 % dilution. Solid lines are best fits to the generalised Debye model as described in the main text. Parameters can be found in Table S5.

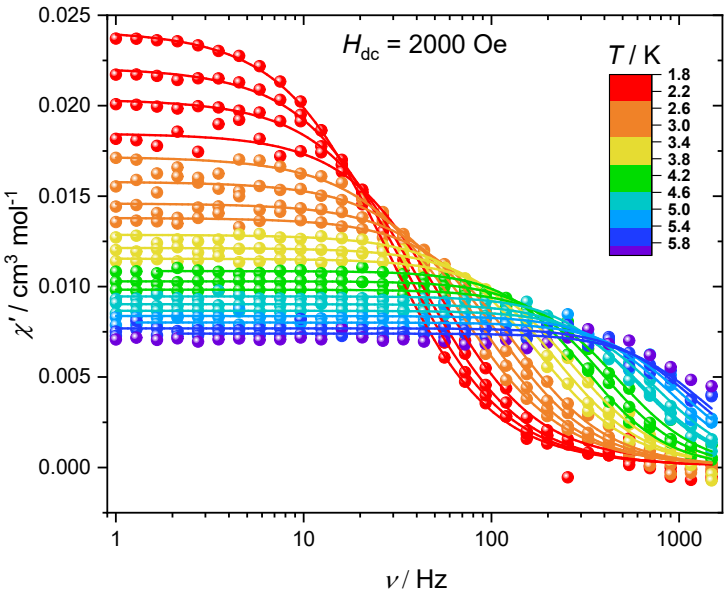

Figure S31. Temperature dependence of the in-phase signal of the ac susceptibility of **Yb@LuL** at 4.2 % dilution. Solid lines are best fits to the generalised Debye model as described in the main text. Parameters can be found in Table S6.

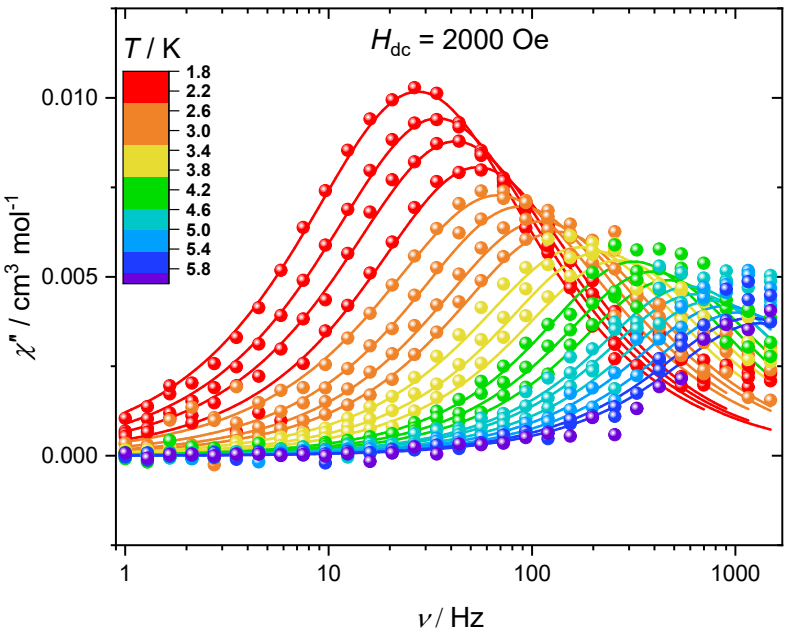

Figure S32. Temperature dependence of the out-of-phase signal of the ac susceptibility of **Yb@LuL** at 4.2 % dilution. Solid lines are best fits to the generalised Debye model as described in the main text. Parameters can be found in Table S6.

Table S4. Best fit parameters (α and τ) for the generalised Debye model fitted to the temperature dependence of the ac magnetic susceptibility of **1** under an applied magnetic field of 2000 Oe.

T **/ K**	τ **/ ms**	α
1.8	0.617	0.132502
1.9	0.545	0.126406
2.0	0.476	0.130576
2.1	0.420	0.130246
2.2	0.384	0.124550
2.3	0.336	0.122576
2.4	0.298	0.123392
2.5	0.266	0.119664
2.6	0.244	0.123105
2.7	0.215	0.120596
2.8	0.195	0.115392
2.9	0.178	0.113132
3.0	0.162	0.105940
3.1	0.148	0.102104
3.2	0.134	0.105400
3.3	0.123	0.087152
3.4	0.117	0.077580

Table S5. Best fit parameters (α and τ) for the generalised Debye model fitted to the temperature dependence of the ac magnetic susceptibility of **1'** under an applied magnetic field of 2000 Oe.

T **/ K**	τ **/ ms**	α
1.8	7.371	0.069869
2.0	5.751	0.052414
2.2	4.553	0.053690
2.4	3.611	0.063772
2.6	2.665	0.043237
2.8	1.975	0.077161
3.0	1.498	0.006180
3.2	1.152	0.000014
3.4	0.839	0.003826
3.6	0.639	0.000001
3.8	0.462	0.000000
4.0	0.378	0.004485
4.2	0.311	0.000000
4.4	0.217	0.000000
4.6	0.206	0.017066
4.8	0.164	0.017789
5.0	0.131	0.031950
5.2	0.151	0.000030

Table S6. Best fit parameters (α and τ) for the generalised Debye model fitted to the temperature dependence of the ac magnetic susceptibility of **Yb@LuL** at 4.2% dilution under an applied magnetic field of 2000 Oe.

T **/ K**	τ **/ ms**	α
1.8	5.793	0.108019
2.0	4.624	0.101124
2.2	3.783	0.094294
2.4	2.942	0.076802
2.6	2.340	0.105816
2.8	1.822	0.080573
3.0	1.440	0.069056
3.2	1.199	0.061864
3.4	0.911	0.063024
3.6	0.733	0.040777
3.8	0.602	0.035873
4.0	0.502	0.000114
4.2	0.407	0.000000
4.4	0.339	0.001090
4.6	0.269	0.000000
4.8	0.250	0.000000
5.0	0.208	0.000000
5.2	0.179	0.000000
5.4	0.152	0.000000
5.6	0.134	0.000000
5.8	0.120	0.000000

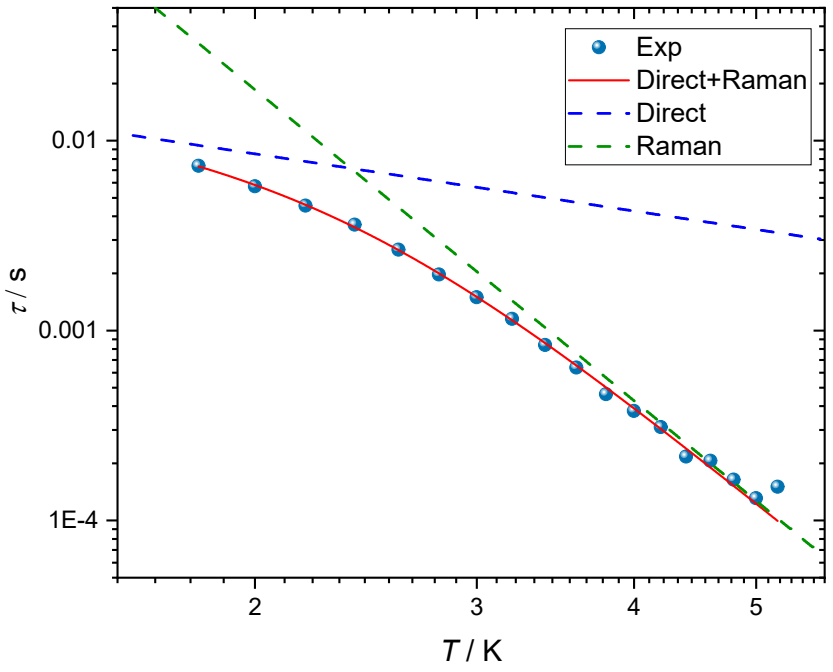

Figure S33. Relaxation times of **1'** at 4.8 % dilution as a function of temperature together with the best fit using a direct and Raman process as described in the main text.

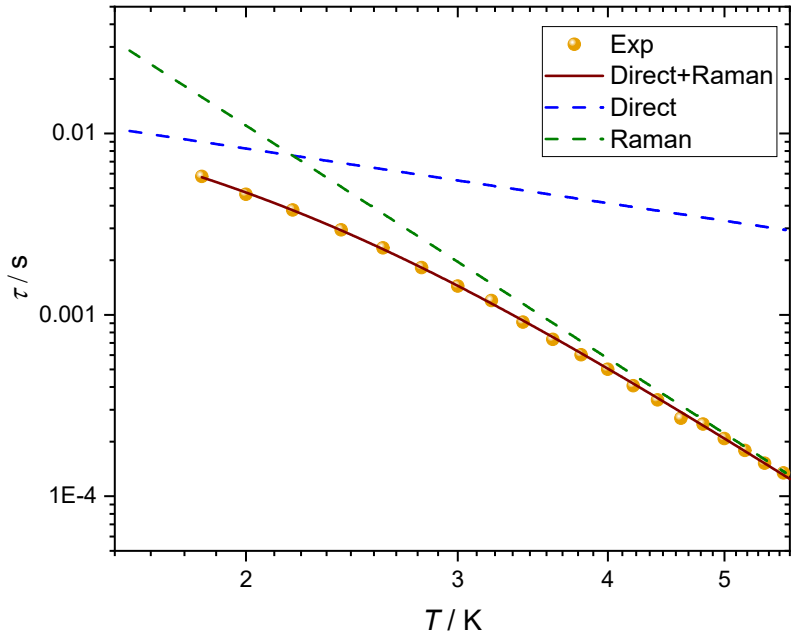

Figure S34. Relaxation time of **Yb@LuL** at 4.2% dilution as a function of temperature together with the best fit using a direct and Raman process as described in the main text.

1. Buch, C. D.; Hansen, S. H.; Tram, C. M.; Mitcov, D.; Piligkos, S., Functionalized Trigonal Lanthanide Complexes: A New Family of 4f Single-Ion Magnets. *Inorg Chem* **2020,** *59* (22), 16328-16340.